

# On the polarizability assessments of ion-based optical clocks

M. D. Barrett,<sup>1,2,\*</sup> K. J. Arnold,<sup>1</sup> and M. S. Safronova<sup>3,4</sup>

<sup>1</sup>Centre for Quantum Technologies, National University of Singapore, 3 Science Drive 2, 117543 Singapore

<sup>2</sup>Department of Physics, National University of Singapore, 2 Science Drive 3, 117551 Singapore

<sup>3</sup>Department of Physics and Astronomy, University of Delaware, Newark, Delaware 19716, USA

<sup>4</sup>Joint Quantum Institute, National Institute of Standards and Technology  
and the University of Maryland, College Park, Maryland, 20742

It is shown that the dynamic differential scalar polarisability of the  $S_{1/2}-D_{5/2}$  transition in  $^{138}\text{Ba}^+$  can be determined to an inaccuracy below 0.5% across a wide wavelength range ( $\lambda > 700$  nm). This can be achieved using measurements for which accurate determination of laser intensity is not required, and most of the required measurements are already in the literature. Measurement of a laser-induced ac-stark shift of the clock transition would then provide an *in situ* measurement of the laser's intensity to the same 0.5% level of inaccuracy, which is not easily achieved by other means. This would allow accurate polarisability measurements for clock transitions in other ions, through comparison with  $^{138}\text{Ba}^+$ . The approach would be equally applicable to  $\text{Sr}^+$  and  $\text{Ca}^+$ , with the latter being immediately applicable to  $\text{Al}^+/\text{Ca}^+$  quantum logic clocks.

PACS numbers: 06.30.Ft, 06.20.fb

The dynamic differential scalar polarisability  $\Delta\alpha_0(\omega)$  of a clock transition is an important quantity to determine. The dc value  $\Delta\alpha_0(0)$  quantifies the blackbody radiation (BBR) shift, and contributes to micromotion shift assessments in ion-based clocks. For ions, the accurate determination of  $\Delta\alpha_0(0)$  is in general difficult. When  $\Delta\alpha_0(0) < 0$ , second-order Doppler and ac-Stark shifts arising from micromotion can be cancelled by operating at a specific trap drive frequency, which depends on  $\Delta\alpha_0(0)$  [1]. As demonstrated with  $\text{Sr}^+$  and  $\text{Ca}^+$ , this has allowed accurate determination of  $\Delta\alpha_0(0)$  through suppression of clock frequency shifts arising from induced micromotion [2, 3]. Other ion-based clocks have needed to rely on some form of extrapolation from measurements in the near-infrared (NIR) [4, 5] and/or by measurement at infrared (IR) wavelengths near to the center of the blackbody spectrum [6–8].

The accuracy of polarizability measurements at NIR or IR wavelengths is limited to the accuracy by which the intensity of the laser at the ion can be determined. This is primarily limited by detector calibration. Depending on the wavelength, detector calibration at the 1-2% level can be difficult, expensive or practically impossible. Even if the detector is accurately calibrated, the mode of the laser field at the ion must be equally well-calibrated, which is complicated by beam aberration and etaloning effects. Consequently, the ability to accurately calibrate  $\Delta\alpha_0(\omega)$  through intensity-independent measurements is an attractive alternative, which would also allow subsequent *in situ* calibration of laser intensities for measurements against other ions. Here it is shown that the simple atomic structure of alkaline-earth ions allows just such an approach. Moreover, most of the required measurements have already been reported in the literature. Although the discussion is focussed on  $^{138}\text{Ba}^+$ , the idea is equally applicable to  $^{88}\text{Sr}^+$  and  $^{40}\text{Ca}^+$ .

For the  $S_{1/2}$  to  $D_{5/2}$  transition in  $^{138}\text{Ba}^+$ ,  $\Delta\alpha_0(\omega)$  is predominately determined by three transitions at 614, 493, and 455 nm with all other contributing transitions having wavelengths below 240 nm. For wavelengths above 700 nm, the ultraviolet (uv) contributions can be well represented by a weak quadratic correction. Consequently, accurate determination of the matrix elements associated with the three dominant poles, together with a characterisation of an overall dc offset, should provide a reasonably accurate representation of  $\Delta\alpha_0(\omega)$  over a wide frequency range.

In table I, contributions to  $\Delta\alpha_0(\omega)$  are tabulated using matrix elements calculated by a linearized coupled-cluster method described in Ref. [9] with the exception of the  $6s - 6p$  transitions which are taken from experiment [10]. The contributions labeled other are obtained using the approach from Refs. [11, 12], after subtracting off leading contributions. Not given in the table are the core polarizability terms as these are the same for the two states and cancel for a differential polarizability. However, valence-core correction terms,  $\alpha_{vc}$ , which compensate for Pauli-principle-violating excitations from the core to the valence shell [13], are included. Theoretical calculations of matrix elements, polarizabilities and their accuracy are discussed in the Supplemental Material [14].

The actual values of the matrix elements and correction terms are not crucial. More important is that the dominant contributions are determined by the three poles at 614, 493, and 455 nm and the rest can be approximated by a weak quadratic form. This is illustrated in Fig. 1, which shows the polarisability curve calculated from the values given in table I and, for comparison, the contribution from the three dominant poles only. For this purpose the ‘other’ contributions have been treated as single poles with the largest possible wavelength for the con-

TABLE I. Contributions to the polarizabilities in  $\text{Ba}^+$ . Dipole matrix elements and polarizability contributions are given in atomic units.

State	Contribution	$\lambda$ (nm)	$D$	$\alpha$
$6s\ ^2S_{1/2}$	$6p\ ^2P_{1/2}$	493.5	3.3251	39.92
	$7p\ ^2P_{1/2}$	202.5	0.061	0.06[-1]
	$8p\ ^2P_{1/2}$	163.0	0.087	0.09[-1]
	$6p\ ^2P_{3/2}$	455.5	4.7017	73.67
	$7p\ ^2P_{3/2}$	200.0	0.087	0.11[-1]
	$8p\ ^2P_{3/2}$	162.2	0.033	0.03[-1]
	Other	< 147.8		0.35[-1]
	$\alpha_{vc}$			-0.51
	Total			113.14
	$5d\ ^2D_{5/2}$	$6p\ ^2P_{3/2}$	614.3	4.103
$7p\ ^2P_{3/2}$		225.5	0.451	0.11
$8p\ ^2P_{3/2}$		178.7	0.223	0.02
Other		< 161.3		0.04
Total ( $J = 3/2$ )				25.39
$4f\ ^2F_{5/2}$		234.8	0.998	0.57
$5f\ ^2F_{5/2}$		193.4	0.220	0.02
$6f\ ^2F_{5/2}$		169.7	0.239	0.02
$7f\ ^2F_{5/2}$		157.4	0.116	0.05[-1]
Other		< 150.5		0.10
Total ( $J = 5/2$ )				0.725
$4f\ ^2F_{7/2}$		233.6	4.475	11.41
$5f\ ^2F_{7/2}$		192.5	1.089	0.56
$6f\ ^2F_{7/2}$		169.4	0.971	0.39
$7f\ ^2F_{7/2}$		157.3	0.932	0.33
Other		< 150.4		2.02
Total ( $J = 7/2$ )				14.71
$\alpha_{vc}$			-0.82	
Total			40.00	

tributing terms used as the pole position in each case. As is evident from the figure, in the region  $\omega \lesssim 0.065$  a.u.

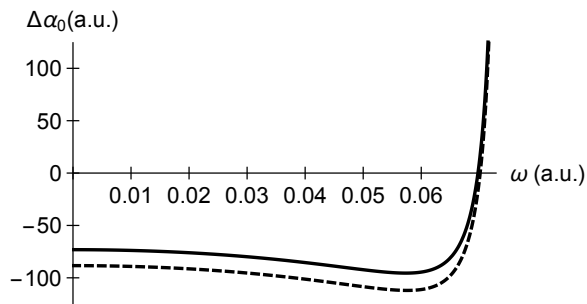


FIG. 1. Plot of the differential scalar polarisability,  $\Delta\alpha_0(\omega)$ . Solid curve is calculated using matrix elements given in table I. Dashed curve is the contribution from the transitions at 455, 493, and 614 nm. Both axes are given in atomic units.

( $\lambda \gtrsim 700$  nm), the remaining contributions provide an essentially constant offset.

For  $\omega \lesssim 0.065$  a.u., contributions from the uv tran-

sitions and  $\alpha_{vc}$  terms can be well approximated by an even-order quadratic polynomial, as can the positive sum of such terms. From the parameterisation

$$c_0 + c_0 \left( \frac{\omega}{\omega_0} \right)^2, \quad (1)$$

it is readily seen that the single pole

$$\frac{c_0}{1 - (\omega/\omega_0)^2}, \quad (2)$$

has the same quadratic expansion as a sum of poles. Thus, a single pole can well approximate the uv contributions and  $\alpha_{vc}$  terms up to second order. Additionally, the single pole will partially capture contributions from higher order terms. Provided there is no significant cancellation of poles, this argument also holds for a differential polarisability. This is the case for  $\text{Ba}^+$ , as the uv terms are dominated by the  $D_{5/2}$  to  $4f\ ^2F_{7/2}$  transition and there is only a few percent contribution from transitions connected to the ground state [15]. It therefore follows that, in the region  $\omega \lesssim 0.065$  a.u.,  $\Delta\alpha_0(\omega)$  can be well approximated by a sum of four poles:

$$\begin{aligned} \Delta\alpha_0(\omega) &= \Delta\alpha_0^{\text{vis}}(\omega) + \Delta\alpha_0^{\text{uv}}(\omega) \\ &\approx \Delta\alpha_0^{\text{vis}}(\omega) + \frac{c_0}{1 - (\omega/\omega_0)^2}, \end{aligned} \quad (3)$$

where  $\Delta\alpha_0^{\text{vis}}(\omega)$  gives the contributions from the 455, 493, and 614 nm transitions, and  $\Delta\alpha_0^{\text{uv}}(\omega)$  the rest.

Mathematically, the approximation given by Eq. 3 can be exceptionally good. Taking  $\Delta\alpha_0(\omega)$  calculated using all contributions given in table I as a representative example,  $c_0$  and  $\omega_0$  can be chosen such that the approximation matches the zero crossing of  $\Delta\alpha_0(\omega)$  and minimizes the discrepancy over the range  $\omega_0 < 0.065$  a.u. This gives  $c_0 = 15.23$  a.u. and  $\omega_0 = 0.2048$  a.u. ( $\lambda_0 = 222.494$  nm), with a maximum fractional discrepancy of  $\sim 2 \times 10^{-5}$  over the frequency range of interest. The agreement only relies on the validity of the single pole approximation to the uv and  $\alpha_{vc}$  terms, which is not dependent on exact values of matrix elements. The practical limitation is set by how well the approximation can be realized.

To experimentally characterize the approximation, the procedure would be to first fix the three main contributions, by determining directly the matrix elements associated with the transitions at 455, 493, and 614 nm, and then to locate the zero crossing to determine the offset. Since the quadratic correction is weak, the quality of the approximation is insensitive to  $\omega_0$ , so it can be fixed to a value determined by theory. With  $\omega_0$  fixed,  $c_0$  would then be chosen so that the zero crossing for the approximation matches the measured position of the zero crossing at  $\omega \approx 0.07$  a.u. ( $\lambda \approx 653$  nm). It then remains to determine how good the approximation is, taking into account reasonable experimental measurements and theoretical estimates of  $\omega_0$ .

High accuracy determination of individual matrix elements has been achieved in a number of different ways. Precision measurement of excited state lifetimes [16–18] and branching fractions [19–21] give matrix elements with inaccuracies  $\lesssim 1\%$ . For  $^{40}\text{Ca}^+$ , comparison of off-resonant scattering rates and Stark shifts enabled the determination of matrix elements with inaccuracies at the 0.1% level [22]. For  $\text{Ba}^+$ , resonant excitation stark ionisation spectroscopy has been used to determine matrix elements for the 493 and 455 nm transitions with reported inaccuracies of 0.05% [10]. The latter measurements, combined with branching fractions given in [20], would determine the matrix element  $\langle P_{3/2} \| r \| D_{5/2} \rangle$  to an inaccuracy of  $\sim 0.3\%$ .

Improved accuracy of  $\langle P_{3/2} \| r \| D_{5/2} \rangle$  should be readily achievable. Optical pumping into  $D_{3/2}$  followed by depumping with 585 nm light, which couples  $D_{3/2}$  to  $P_{3/2}$ , would optically pump the atom into  $S_{1/2}$  and  $D_{5/2}$  with probability  $p \sim 0.66$  and  $1 - p$ , respectively. Measurement of  $p$  would then provide the desired matrix element via the relation

$$\frac{\langle P_{3/2} \| r \| D_{5/2} \rangle}{\langle P_{3/2} \| r \| S_{1/2} \rangle} = \left( \frac{\omega_{455}}{\omega_{614}} \right)^{3/2} \sqrt{\frac{1-p}{p}}. \quad (4)$$

The fractional inaccuracy in the determination of  $\langle P_{3/2} \| r \| D_{5/2} \rangle$  due to projection noise in a measurement of  $p$  is then  $\sim 1/\sqrt{N}$ , where  $N$  is the number of measurements. This method is insensitive to laser intensities, polarisation, and detunings. Since  $D_{5/2}$  has a lifetime of  $\sim 30$  s, state detection errors can be negligibly small and accuracy would be ultimately limited by the accuracy of  $\langle P_{3/2} \| r \| S_{1/2} \rangle$ . Thus it is not unreasonable to suggest that this contribution could also be determined to an inaccuracy of 0.1%.

For a given value of  $\omega_0$ ,  $c_0$  can be set by determining the zero crossing near 653 nm. In this region there is a large contribution from the tensor polarisability, but this can be heavily suppressed by appropriate orientation of the magnetic field with respect to the laser polarisation, as done in recent experiments with  $\text{Lu}^+$  [6], and by averaging over Zeeman pairs, as done with  $\text{Sr}^+$  [23]. Also, determination of the zero crossing does not require an accurate assessment of laser intensity. At  $\pm 500$  GHz from the zero crossing,  $\Delta\alpha_0(\omega) \approx \pm 3$  a.u., which should enable a readily measurable stark shift. Linear interpolation of the two points would then give an estimate of the zero point. Provided the intensity was stabilised to a fixed value for both measurements, accuracy of this approach would be limited by the curvature of  $\alpha_0(\omega)$  within this region, which would bias the result by an estimated  $\approx -10$  GHz. Based on this, 20 GHz should be an achievable uncertainty for the zero crossing.

Determination of  $\omega_0$  would rely on theoretical calculations. From Eq. 3, the zero crossing  $\Delta\alpha_0(\omega') = 0$  gives

$$\Delta\alpha_0^{\text{uv}}(\omega') = -\Delta\alpha_0^{\text{vis}}(\omega') \approx \frac{c_0}{1 - (\omega'/\omega_0)^2}. \quad (5)$$

Since  $\Delta\alpha_0^{\text{vis}}(\omega)$  can be determined accurately by independent measurements, locating the zero crossing constitutes a measurement of  $\Delta\alpha_0^{\text{uv}}(\omega')$ . Extrapolating this measurement to dc based on the theoretical representation of  $\Delta\alpha_0^{\text{uv}}(\omega)$  determines  $c_0$ , and the above equation can be then used to determine  $\omega_0$ . This is very similar to the assessment procedure for the blackbody radiation shift in the  $\text{Al}^+$  clock [5, 24]. However, in this case, the accuracy of the measurement  $\Delta\alpha_0^{\text{uv}}(\omega')$  can be assumed sufficiently precise that it does not contribute to the uncertainty in the extrapolation.

The procedure used for  $\text{Al}^+$  is problematic in this case as it is not clear how to choose the expansion parameter used in that approach. Instead, the measurement is treated as a projection to constrain the allowable variation of matrix elements. Specifically,  $\Delta\alpha_0^{\text{uv}}(\omega)$  is first written in the vector form

$$\Delta\alpha_0^{\text{uv}}(\omega) = \sum_k \frac{c_k}{1 - (\omega/\omega_k)^2} = \mathbf{f}(\omega) \cdot \mathbf{c} \quad (6)$$

where the  $k^{\text{th}}$  component of  $\mathbf{f}(\omega)$  is  $1/(1 - (\omega/\omega_k)^2)$ . Since transition frequencies are generally well-known,  $\mathbf{f}(\omega)$  is practically exact. The coefficients  $\mathbf{c}$  have theoretical estimates  $\mathbf{c}_0$ , with an uncertainty  $\delta\mathbf{c}$ . To find the allowable variation in  $\Delta\alpha_0^{\text{uv}}(0)$  consistent with the measurement  $\Delta\alpha_0^{\text{uv}}(\omega')$ ,  $\mathbf{f}(0)$  is written as a projection onto  $\mathbf{f}(\omega')$  and an orthogonal unit vector  $\hat{\mathbf{n}}$ , i.e.  $\mathbf{f}(0) = a_1 \mathbf{f}(\omega') + a_2 \hat{\mathbf{n}}$ , which gives

$$\begin{aligned} \Delta\alpha_0^{\text{uv}}(0) &= \mathbf{f}(0) \cdot \mathbf{c} \\ &= a_1 \Delta\alpha_0^{\text{uv}}(\omega') + a_2 \hat{\mathbf{n}} \cdot \mathbf{c}_0 + a_2 \hat{\mathbf{n}} \cdot \delta\mathbf{c}. \end{aligned} \quad (7)$$

The first term is the contribution determined from the measurement, the second term is the theoretically estimated offset between measured and dc values, and the final term determines the error due to the uncertainty in  $\mathbf{c}$ . Assuming that the uncertainties in the matrix elements are independent, this is simply a weighted sum of independent random variables.

Using the above approach and the values in table I, the position of the approximating pole is found to be 222(5) nm, where we have used a 4% uncertainty in the two  $4f$  contributions and a 100% uncertainty in all others. As before, the contributions labelled ‘other’ have been treated as single poles. Consequently, the errors in the contributions from these terms are assumed correlated. Correlation is also assumed for the errors in the  $nF_{5/2}$  and  $nF_{7/2}$  contributions as these are expected to be related. The assumed frequency dependence of the ‘other’ terms does not significantly affect the uncertainty derived in  $\omega_0$ . Therefore,  $\pm 5$  nm is taken as a reasonable uncertainty for the pole placement.

It should be noted that location of the zero crossing would need to be consistent with that estimated from theory, which we calculate to be 653.0(1.3) nm. If this were not the case, there would be no justification for asserting the validity of an estimate of  $\omega_0$ . However, such

an inconsistency would be rather surprising, given the agreement between theory and experiment for matrix elements [10], branching ratios [20, 21], and even  $\Delta\alpha_0(0)$  [25], although the latter does have a large uncertainty.

To illustrate the sensitivity to the various error contributions, the fractional difference between  $\Delta\alpha_0(\omega)$  calculated using all contributions and the approximation given in Eq. 3 for various errors is plotted in Fig. 2. The solid curve is the error introduced with a fractional decrease of  $10^{-3}$  in the 614-nm contribution, the dashed curve is the error contribution if the uv pole is shifted to 217.5 nm, and the dotted curve is the error contribution if the zero crossing is underestimated by 20 GHz. Each curve scales almost linearly with the stated error, such that the result of a change in sign of an error can be approximated by a reflection of the associated curve about the horizontal axis. Errors arising from the 455 and 493 transitions have been omitted as they are smaller by a factor of  $\sim 3$  than that from the 614-nm transition. This is due to the relative position of the transition with respect to the zero crossing. Adding errors in quadrature, including those from the 455 and 493 poles, gives a maximum error of 0.32% over the entire region from dc to  $\omega = 0.065$  a.u. ( $\sim 700$  nm).

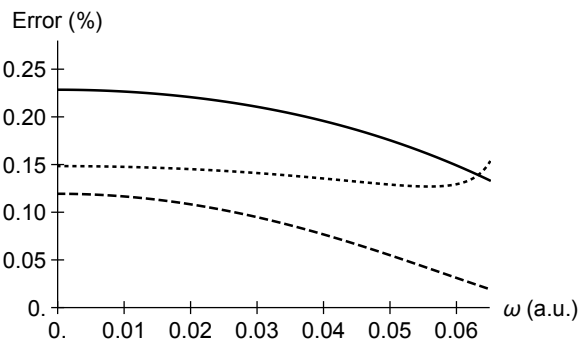


FIG. 2. Plot of the percentage error contributions between a full calculation of  $\Delta\alpha_0(\omega)$  and the approximate expression given in Eq. 3 as a function of the angular frequency  $\omega$  given in atomic units. The solid curve is the error contribution if the pole strength for the 614 nm transition is decreased by 0.1%. The dashed curve is the error contribution if the uv pole is shifted by 5 nm to 217.5 nm. The dotted curve is the error contribution if the zero-crossing is underestimated by 20 GHz.

As already noted, the reduced matrix elements  $\langle P_{3/2} || r || S_{1/2} \rangle$  and  $\langle P_{1/2} || r || S_{1/2} \rangle$  have already been reported in the literature with inaccuracies of  $\sim 0.05\%$  [10]. Hence, all that remains is an improved measurement of the branching fraction  $p$  and location of the zero crossing near 653 nm. In addition,  $\Delta\alpha_0(0) < 0$ , which should allow a high accuracy measurement of  $\Delta\alpha_0(0)$  as done with  $\text{Sr}^+$  and  $\text{Ca}^+$  [2, 3]. This would provide a rigorous consistency check among multiple precision measurements and an experimental assessment of  $\omega_0$ .

In summary, we have shown that the dynamic differential scalar polarisability,  $\Delta\alpha_0(\omega)$ , of the  $S_{1/2} - D_{5/2}$  transition in  $^{138}\text{Ba}^+$  can be determined to an inaccuracy below 0.5% across a wide wavelength range ( $\lambda > 700$  nm). Moreover, the determination can be obtained using measurements that do not require accurate determination of laser intensities and some of the required measurements have already been reported in the literature. Although the method relies on a theoretical estimate of an effective pole position  $\omega_0$ , the resulting approximation to  $\Delta\alpha_0(\omega)$  is relatively insensitive to this value such that this is unlikely to be a significant limitation.

The methodology proposed here would also be applicable to  $\text{Sr}^+$  and  $\text{Ca}^+$ . For these cases, uv transitions are deeper in the uv making the approximation less sensitive to the choice of  $\omega_0$ . In the case of  $\text{Ca}^+$ , an accurate measurement of the  $\langle P_{1/2} || r || S_{1/2} \rangle$  matrix element has been reported [22] and  $\langle P_{3/2} || r || S_{1/2} \rangle$  can be well-approximated by  $\langle P_{1/2} || r || S_{1/2} \rangle \sqrt{2}$  [26]. Together with the branching fractions reported in [27], and the recent high accuracy determination of  $\Delta\alpha_0(0)$  [3], a calibration of the polarizability curve to  $\lesssim 1\%$  could be done. Determination of the zero crossing, which we estimate to be at 297.5(2) THz, would provide a consistency check of the methodology.

The case of  $\text{Ca}^+$  is of particular relevance to the  $\text{Al}^+$  clock, for which the uncertainty in  $\Delta\alpha_0(0)$  is now a significant contribution to the error budget. Measurement of this quantity has only been carried out twice and both rely on extrapolation from a single measurement point [5, 24]. It is therefore desirable to provide an independent assessment. Clock implementations utilizing  $\text{Ca}^+$  as the logic ion would allow accurate calibration of a laser intensity at multiple wavelengths and improved measurements of  $\Delta\alpha_0(\omega)$  for  $\text{Al}^+$ . For wavelengths above 780 nm, the differential scalar polarizability of the  $\text{Al}^+$  clock transition is well approximated by a quadratic form and even two measurements of  $\Delta\alpha_0(\omega)$  in the NIR would allow a more accurate extrapolation to dc.

Measurements proposed in this work will also provide benchmarks for matrix elements involving 4f states, as needed in calculations for highly-charged ions. In addition, they will provide a precision test of methods to compute polarizability contributions from highly-excited states, which will be useful in establishing theoretical uncertainties of predicted polarizabilities in other systems.

This work is supported by the National Research Foundation, Prime Ministers Office, Singapore and the Ministry of Education, Singapore under the Research Centres of Excellence programme, and by A\*STAR SERC 2015 Public Sector Research Funding (PSF) Grant (SERC Project No: 1521200080). This research was performed in part under the sponsorship of the Office of Naval Research, Grant No. N00014-17-1-2252.

\* phybmd@nus.edu.sg

- [1] DJ Berkeland, JD Miller, James C Bergquist, Wayne M Itano, and David J Wineland. Minimization of ion micromotion in a paul trap. *Journal of applied physics*, 83(10):5025–5033, 1998.
- [2] Pierre Dubé, Alan A Madej, Maria Tibbo, and John E Bernard. High-accuracy measurement of the differential scalar polarizability of a  $^{88}\text{Sr}^+$  clock using the time-dilation effect. *Physical review letters*, 112(17):173002, 2014.
- [3] Y Huang, H Guan, M Zeng, L Tang, and K Gao.  $^{40}\text{Ca}^+$  ion optical clock with micromotion induced shifts below  $1 \times 10^{-18}$ . *Physical Review A*, 99(1):011401, 2019.
- [4] N Huntemann, C Sanner, B Lipphardt, Chr Tamm, and E Peik. Single-ion atomic clock with  $3 \times 10^{-18}$  systematic uncertainty. *Physical review letters*, 116(6):063001, 2016.
- [5] T Rosenband, Wayne M Itano, PO Schmidt, DB Hume, JCJ Koelemeij, James C Bergquist, and David J Wineland. Blackbody radiation shift of the  $^{27}\text{Al}^+ \ ^1S_0 \rightarrow \ ^3P_0$  transition. In *Proceedings of the 20th European Frequency and Time Forum*, pages 289–292. IEEE, 2006.
- [6] KJ Arnold, R Kaewuam, A Roy, TR Tan, and MD Barrett. Blackbody radiation shift assessment for a lutetium ion clock. *Nature communications*, 9, 2018.
- [7] KJ Arnold, R Kaewuam, TR Tan, SG Porsev, MS Safronova, and MD Barrett. Dynamic polarizability measurements with  $^{176}\text{Lu}^+$ . *Physical Review A*, 99(1), 2019.
- [8] CFA Baynham, EA Curtis, RM Godun, JM Jones, PBR Nisbet-Jones, PEG Baird, K Bongs, P Gill, T Fordell, T Hieta, et al. Measurement of differential polarizabilities at a mid-infrared wavelength in  $^{171}\text{Yb}^+$ . *arXiv preprint arXiv:1801.10134*, 2018.
- [9] MS Safronova and WR Johnson. All-order methods for relativistic atomic structure calculations. *Advances in atomic, molecular, and optical physics*, 55:191–233, 2008.
- [10] Shannon L Woods, ME Hanni, SR Lundeen, and Erica L Snow. Dipole transition strengths in  $\text{Ba}^+$  from rydberg fine-structure measurements in Ba and  $\text{Ba}^+$ . *Physical Review A*, 82(1):012506, 2010.
- [11] MS Safronova, MG Kozlov, WR Johnson, and Dansha Jiang. Development of a configuration-interaction plus all-order method for atomic calculations. *Physical Review A*, 80(1):012516, 2009.
- [12] SG Porsev, Yu G Rakhlina, and MG Kozlov. Electric-dipole amplitudes, lifetimes, and polarizabilities of the low-lying levels of atomic ytterbium. *Physical Review A*, 60(4):2781, 1999.
- [13] MS Safronova, WR Johnson, and A Derevianko. Relativistic many-body calculations of energy levels, hyperfine constants, electric-dipole matrix elements, and static polarizabilities for alkali-metal atoms. *Physical Review A*, 60(6):4476, 1999.
- [14] See Supplemental Material at for details of the theoretical calculations.
- [15] E Iskrenova-Tchoukova and MS Safronova. Theoretical study of lifetimes and polarizabilities in  $\text{Ba}^+$ . *Physical Review A*, 78(1):012508, 2008.
- [16] S Olmschenk, D Hayes, DN Matsukevich, P Maunz, DL Moehring, KC Younge, and C Monroe. Precision measurement of the lifetime of the  $6p \ ^2P_{1/2}$  level of Yb. *Phys. Rev. A*, 73:023413, 2006.
- [17] HJ Andrä, A Gaupp, and W Wittmann. New method for precision lifetime measurements by laser excitation of fast-moving atoms. *Physical Review Letters*, 31(8):501, 1973.
- [18] Jian Jin and DA Church. Precision lifetimes for the  $\text{Ca}^+ \ 4p \ ^2P$  levels: Experiment challenges theory at the 1% level. *Physical review letters*, 70(21):3213, 1993.
- [19] Michael Ramm, Thaned Pruttivarasin, Mark Kokish, Ishan Talukdar, and Hartmut Häffner. Precision measurement method for branching fractions of excited  $P_{1/2}$  states applied to  $^{40}\text{Ca}^+$ . *Physical review letters*, 111(2):023004, 2013.
- [20] Tarun Dutta, Debashis De Munshi, Dahyun Yum, Riadh Rebhi, and Manas Mukherjee. An exacting transition probability measurement—a direct test of atomic many-body theories. *Scientific reports*, 6:29772, 2016.
- [21] D De Munshi, T Dutta, R Rebhi, and M Mukherjee. Precision measurement of branching fractions of  $^{138}\text{Ba}^+$ : Testing many-body theories below the 1% level. *Physical Review A*, 91(4):040501, 2015.
- [22] M Hettrich, T Ruster, H Kaufmann, CF Roos, CT Schmiegelow, F Schmidt-Kaler, and UG Poschinger. Measurement of dipole matrix elements with a single trapped ion. *Physical review letters*, 115(14):143003, 2015.
- [23] P Dubé, AA Madej, JE Bernard, L Marmet, J-S Boulanger, and S Cundy. Electric quadrupole shift cancellation in single-ion optical frequency standards. *Phys. Rev. Lett.*, 95(3):033001, 2005.
- [24] SM Brewer, J-S Chen, AM Hankin, ER Clements, CW Chou, DJ Wineland, DB Hume, and DR Leibrandt. An  $^{27}\text{Al}^+$  quantum-logic clock with systematic uncertainty below  $10^{-18}$ . *arXiv preprint arXiv:1902.07694*, 2019.
- [25] Nan Yu, X Zhao, H Dehmelt, and W Nagourney. Stark shift of a single barium ion and potential application to zero-point confinement in a rf trap. *Physical Review A*, 50(3):2738, 1994.
- [26] MS Safronova and UI Safronova. Blackbody radiation shift, multipole polarizabilities, oscillator strengths, lifetimes, hyperfine constants, and excitation energies in  $\text{Ca}^+$ . *Physical Review A*, 83(1):012503, 2011.
- [27] R Gerritsma, G Kirchmair, F Zähringer, J Benhelm, R Blatt, and CF Roos. Precision measurement of the branching fractions of the  $4p^2 \ P_{3/2}$  decay of Ca II. *The European Physical Journal D*, 50(1):13–19, 2008.

## Supplemental Material Calculations of Ba<sup>+</sup> polarizabilities

The valence parts of the scalar,  $\alpha_0$ , and tensor,  $\alpha_2$ , polarizabilities of Ba<sup>+</sup> levels may be calculated using the sum-over-states expressions [2]:

$$\begin{aligned}\alpha_0^v(\omega) &= \frac{2}{3(2j_v + 1)} \sum_k \frac{\langle k \| D \| v \rangle^2 \Delta E}{\Delta E^2 - \omega^2}, \text{ and} \\ \alpha_2^v(\omega) &= -4C \sum_k (-1)^{j_v + j_k + 1} \begin{Bmatrix} j_v & 1 & j_k \\ 1 & j_v & 2 \end{Bmatrix} \\ &\quad \times \frac{\langle k \| D \| v \rangle^2 \Delta E}{\Delta E^2 - \omega^2},\end{aligned}\quad (1)$$

where  $C$  is given by

$$C = \left( \frac{5j_v(2j_v - 1)}{6(j_v + 1)(2j_v + 1)(2j_v + 3)} \right)^{1/2}.$$

Here,  $\delta_E = E_k - E_v$ ,  $\langle i \| D \| j \rangle$  are reduced electric-dipole matrix elements and the sum over intermediate  $k$  states includes contributions from all transitions allowed by the electric-dipole selection rules. We use a finite B-spline basis set which make this sum finite. The first few terms give dominant contributions and respective matrix elements have to be calculated with the highest possible accuracy. We use a linearised coupled-cluster (LCC) method [3] that includes dominant classes of correlation corrections to all orders of perturbation theory. This method was used for the prediction of the Ca<sup>+</sup> [4] and Sr<sup>+</sup> [5] differential clock state scalar polarizabilities and subsequent measurements confirmed the accuracy of this approach.

Four different LCC calculations were carried out: two *ab initio* calculations that include single-double excitations (SD) and additional partial triple contributions (SDpT), and two other calculations, labeled SD<sub>sc</sub> and SDpT<sub>sc</sub>, where higher excitations are estimated using a scaling procedure. Details of the method and a description of the scaling procedures is given in [3]. The all-order results are given in Table I. We also list lowest order Dirac Hartree-Fock (DHF) and random phase approximation (RPA) values to demonstrate the size of the correlations corrections. In addition, the matrix elements that include RPA and corrections to the one-body part of the Hamiltonian ( $\Sigma_1$ ) are included. Two ( $\Sigma_1$ ) calculations were carried out; one to second order of perturbation theory, and the other to all orders. These calculations follow the methods described in [6], with the valence-valence part of the calculations omitted, as Ba<sup>+</sup> has a single valence electron. We use these methods to evaluate polarizability contributions from the higher states and it is important to compared these results to the final LCC values. The uncertainties of the  $5d_{5/2} - np_{3/2}$  and

$5d_{5/2} - 4f_j$  matrix elements are determined as the maximum difference of the final and three other LCC values.

Correlations corrections are very large for the  $nf$  Ba<sup>+</sup> states, which causes convergence issues in the LCC calculations that cannot be fixed with usual stabiliser methods [7]. We use additional fitting for the  $nf$  states to resolve this issue ensuring correct energies after the termination of the LCC calculations. We still find very large differences between the SD and SDpT  $5d_{5/2} - 5f_j$  and  $5d_{5/2} - 6f_j$  values. As a result, we assign a 100% uncertainty to the corresponding  $5d_{5/2}$  polarizability contributions based on the spread of LCC matrix element values.

The contributions to the  $6s$  static and dynamic polarizabilities at  $\lambda = 653$  nm are given in Table II. Experimental values from [1] obtained using the resonant excitation Stark ionization spectroscopy technique are used for the  $6s - 6p$  matrix elements. Experimental energies are used in the calculation of main contributions for all polarizability calculations. The contribution of states with  $n > 8$  is very small and is calculated in the RPA. A maximum difference of the DHF and RPA tail values for the  $np_{1/2}$  and  $np_{3/2}$  cases is taken to be the tail uncertainty. The ionic core polarizability and small correction accounting for the occupied valence orbital ( $\alpha_{vc}$ ) are also calculated in the RPA.

Because of significant contributions from the higher  $nf_{7/2}$  states to the  $5d_{5/2}$  polarizability, we use a more accurate method to evaluate the tail for the  $5d_{5/2}$  polarizability. The tail includes the contribution of the  $(n > 8)p_{3/2}$  and  $(n > 7)f_j$  states. Instead of using the sum-over-states approach we solve the inhomogeneous equation of perturbation theory in the valence space, which is approximated as

$$(E_v - H_{\text{eff}})|\Psi(v, M')\rangle = D_{\text{eff},q}|\Psi_0(v, J, M)\rangle \quad (2)$$

for a state  $v$  with the total angular momentum  $J$  and projection  $M$  [8] and then use resulting wave functions for the polarizability calculations. The  $H_{\text{eff}}$  term includes either second-order ( $\Sigma_1^{(2)}$ ) or the all-order ( $\Sigma_1^{(all)}$ ) corrections as described in [6], the effective dipole operator  $D_{\text{eff}}$  includes random phase approximation (RPA) corrections. Tail results, calculated in various approximations, are listed in Table III. We find results to be very stable with the approximation and assign the spread of the values as the uncertainty.

The crossing of the  $6s$  and  $5d_{5/2}$  static polarizabilities is found to be 653.0(1.3) nm, where the uncertainty is predominately due to the uncertainty of the  $5d_{5/2}$  contributions. As seen in Table IV, the uncertainty is almost entirely from the  $5d_{5/2} - 6p_{3/2}$  contribution. Thus we can

TABLE I. Absolute values of the reduced matrix elements contributing to the  $5d_{5/2}$  polarizability calculated in different approximations (in a.u.). DHF - Dirac Hartree-Fock lowest order, RPA - random phase approximation,  $\text{RPA}+\Sigma_1^{(2,\text{all})}$  include correlation potential in second and all-order approximations, respectively. The all-order single-double (SD) and single-double + partial triple (SDpT) results are listed in SD and SDpT columns, corresponding scaled vales are listed in the  $\text{SD}_{\text{sc}}$  and  $\text{SDpT}_{\text{sc}}$  columns. Uncertainties are given in parentheses. \*See text for a discission of uncertainties.

Transition	DHF	RPA	$\text{RPA}+\Sigma_1^{(2)}$	$\text{RPA}+\Sigma_1^{(\text{all})}$	SD	SDpT	$\text{SD}_{\text{sc}}$	$\text{SDpT}_{\text{sc}}$	Final
$5d_{5/2} - 6p_{3/2}$	4.993	4.592	4.015	4.090	4.103	4.163	4.137	4.122	4.103(50)
$5d_{5/2} - 7p_{3/2}$	0.546	0.368	0.424	0.422	0.451	0.450	0.446	0.457	0.451(9)
$5d_{5/2} - 8p_{3/2}$	0.299	0.187	0.207	0.205	0.223	0.224	0.221	0.225	0.223(4)
$5d_{5/2} - 4f_{5/2}$	1.145	1.040	0.955	0.986	0.998	1.012	1.011	1.009	0.998(20)
$5d_{5/2} - 5f_{5/2}$	0.629	0.537	0.159	0.102	0.016	0.210	0.027	0.220	0.220*
$5d_{5/2} - 6f_{5/2}$	0.406	0.330	0.239	0.262	0.236	0.018	0.239	0.024	0.239*
$5d_{5/2} - 7f_{5/2}$	0.286	0.223	0.195	0.221	0.113	0.116	0.116	0.108	0.12(6)
$5d_{5/2} - 4f_{7/2}$	5.128	4.655	4.335	4.464	4.475	4.540	4.521	4.523	4.475(90)
$5d_{5/2} - 5f_{7/2}$	2.812	2.402	0.520	0.236	0.130	1.049	0.085	1.089	1.089*
$5d_{5/2} - 6f_{7/2}$	1.815	1.475	0.999	1.086	0.961	0.170	0.971	0.186	0.971*
$5d_{5/2} - 7f_{7/2}$	1.278	0.996	0.838	0.952	0.922	0.429	0.932	0.388	0.93(54)

TABLE II. Contributions to the static scalar  $6s$  polarizability  $\alpha_0(0)$  and dynamic polarizability at  $\lambda = 653.0$  nm. The absolute values of the  $6s - np$  reduced matrix elements (in a.u.) are also listed in the column labelled ME. Uncertainties are given in parentheses.

Contribution	ME	$\alpha_0(0)$	$\alpha_0(\omega)$
$6p_{1/2}$	3.3251(21) <sup>(a)</sup>	39.921(48)	93.11(11)
$7p_{1/2}$	0.061	0.006	0.006
$8p_{1/2}$	0.087	0.009	0.010
$(n > 8)p_{1/2}$		0.030(20)	0.030(20)
$6p_{3/2}$	4.7017(27) <sup>(a)</sup>	73.670(88)	143.51(17)
$7p_{3/2}$	0.087	0.011	0.012
$8p_{3/2}$	0.033	0.003	0.001
$(n > 8)p_{3/2}$	0.0057	0.005(20)	0.005(20)
$\alpha_{vc}$		-0.51(13)	-0.51(13)
Sum		113.14(17)	236.17(25)
Core		10.6(5)	10.6(5)
Final		123.7(5)	246.8(6)

<sup>(a)</sup>Ref. [1].

TABLE III. The tail contribution to the static scalar polarizability of the  $5d_{5/2}$  state calculated in different approximations (in a.u.). The contributions from the  $(n > 8)p_{3/2}$  and  $(n > 7)f_j$  higher states are included. The same designations are used as in Table I.

Approximation	Tail
DHF	2.498
RPA	1.817
RPA+ $\Sigma_1^{(2)}$	2.249
RPA+ $\Sigma_1^{\text{all}}$	2.156
Final	2.16(34)

expect this to be improved once a more accurate determination of the  $5d_{5/2} - 6p_{3/2}$  matrix element is made. For completeness we note that the static tensor polarizability and the dynamic tensor polarizability at 653 nm are calculated to be  $-29.8(7)$  a.u. and  $-225(5)$  a.u., respectively.

TABLE IV. Contributions to the static scalar  $5d_{5/2}$  polarizability  $\alpha_0(0)$  and dynamic polarizability at  $\lambda = 653.0$  nm. Uncertainties are given in parentheses.

Contribution	$\alpha_0(0)$	$\alpha_0(\omega)$
$6p_{3/2}$	25.22(61)	219.5(5.3)
$7p_{3/2}$	0.112(5)	0.127(5)
$8p_{3/2}$	0.022(1)	0.023(1)
$(n > 8)p_{3/2}$	0.037	0.038
$4f_{5/2}$	0.570(23)	0.655(26)
$5f_{5/2}$	0.023(23)	0.025(25)
$6f_{5/2}$	0.024(24)	0.025(25)
$7f_{5/2}$	0.005(5)	0.006(6)
$(n > 7)f_{5/2}$	0.103	0.106
$4f_{7/2}$	11.41(46)	13.08(52)
$5f_{7/2}$	0.56(56)	0.61(61)
$6f_{7/2}$	0.39(39)	0.42(42)
$7f_{7/2}$	0.33(33)	0.35(35)
$(n > 7)f_{7/2}$	2.02	2.09
Total tail	2.16(34)	2.23(34)
$\alpha_{vc}$	-0.82(3)	-0.82(3)
Total	40.0(1.1)	236.2(5.4)
Core	10.6(5)	10.6(5)
Final	50.6(1.2)	246.8(5.4)

- [7] H. Gharibnejad, E. Eliav, M. S. Safronova, and A. Derevianko, Phys. Rev. A **83**, 052502 (2011).  
[8] S. G. Porsev, Yu. G. Rakhлина, and M. G. Kozlov, Phys. Rev. A **60**, 2781 (1999).

- [1] S. L. Woods, M. E. Hanni, S. R. Lundeen, and E. L. Snow, Phys. Rev. A **82**, 012506 (2010).  
[2] J. Mitroy, M. S. Safronova, and Charles W. Clark, J. Phys. B **43**, 202001 (2010).  
[3] M. S. Safronova and W. R. Johnson, Adv. At. Mol. Opt. Phys. **55**, 191 (2008).  
[4] B. Arora, M. S. Safronova, and C. W. Clark, Phys. Rev. A **76**, 064501 (2007).  
[5] D. Jiang, B. Arora, M. S. Safronova, and C. W. Clark, J. Phys. B **42**, 154020 (2009).  
[6] M. S. Safronova, M. G. Kozlov, W. R. Johnson, and D. Jiang, Phys. Rev. A **80** (2009).